Density functional study of the electronic structure and magnetism of LaFeAsO alloyed with Zn

Lijun Zhang and D. J. Singh
Materials Science and Technology Division, Oak Ridge National Laboratory, Oak Ridge, Tennessee 37831-6114, USA
(Received 12 October 2009; revised manuscript received 24 November 2009; published 23 December 2009)

We report first-principles supercell investigations of $LaFe_{1-x}Zn_xAsO$. These are discussed in relation to existing experimental data on Zn-doped LaFeAsO. As expected, Zn occurs in a d^{10} configuration in the alloy, similar to the pure Zn compound LaZnAsO. This is highly disruptive to the electronic structure of LaFeAsO near the Fermi energy, which is heavily derived from Fe *d* states. This favors localization and the formation of local moments on the Fe atoms near the Zn.

DOI: 10.1103/PhysRevB.80.214530 PACS number(s): 74.25.Jb, 71.20.Be

I. INTRODUCTION

The discovery of high-temperature superconductivity[1] in proximity to magnetism in a series of Fe-based compounds[1–4] provides an interesting contrast to the cuprate superconductors. Certain features, such as the nearness to antiferromagnetic phases, suggest similarities while others, especially the apparently weaker correlations based on spectroscopy[5,6] and the conspicuous absence of Mott insulators in the phase diagrams[7] suggest important differences.

One remarkable difference between the cuprates and Fe-based superconductors is the effect of alloying on the active transition element site. In cuprates, alloying on the Cu site is highly detrimental to superconductivity. For example, even low level substitutions of the Cu^{2+} ions by nonmagnetic Zn^{2+} destroy superconductivity.[8–10] Similarly, a strong suppression of the critical temperature T_c is found with other substitutions, including Fe, Co, and Ni.[9] On the other hand, superconductivity can be induced in the Fe-based materials using substitutions on the Fe site of the undoped parent compounds. These substitutionals can be dopants, such as Co or Ni[11–14] or even certain 4*d* and 5*d* transition elements,[15–18] including Ru, which apparently acts to suppress the antiferromagnetic state without providing doping.[19] This relates to another difference between cuprates and the Fe-based materials. In the Fe-based materials suppression of the magnetic order, e.g., by pressure is sufficient to produce superconductivity[20] while in contrast doping seems to be essential in the cuprates. This suggests a more intimate connection between the magnetic and superconducting phases in the Fe-based materials where both these phases are metallic. A possible implication is that because of the strong correlations in them the cuprates, while conducting, are closer to localization than the Fe-based materials so that at least for some range of substitutions the electronic structures of the Fe-based materials behave as coherent alloys while the cuprates tend to form localized states when substitutions for Cu are made.

Recently, partial Zn substitution for Fe has been reported in the LaFeAs(O,F) system,[21] with interesting results that may shed light on these differences between cuprates and Fe-based superconductors. Although the Zn^{2+} ions that would be expected in this environment, would not dope the Fe planes (based on nominal Fe^{2+}),[4] even low concentrations of Zn (~5%) suppresses the spin-density wave (SDW). Furthermore, the resistivity becomes insulating and increases with increasing Zn content. Recently, an apparently similar insulating behavior was reported in Cu-doped FeSe although there is no ordered SDW in stoichiometric FeSe.[22–24] Even though the SDW is destroyed by Zn substitution in LaFeAsO, no superconductivity is observed. On the other hand, Zn alloying up to ~10% (beyond which phase separation occurs) in doped superconducting $LaFeAsO_{0.9}F_{0.1}$ does not strongly effect the superconductivity, although there is a conflicting report claiming a strong suppression of T_c with Zn substitution.[25] In any case, there is a dramatic effect on the SDW but perhaps not on the superconducting phase.

The purpose of this paper is to study the effect of Zn alloying on the electronic structure of LaFeAsO in order to shed light on the questions raised by the experimental studies mentioned above. We note that LaZnAsO and LaZnPO have been experimentally synthesized and characterized as semiconductors with the band gap of 1.3–2.3 eV.[26–28] Prior electronic-structure calculations on LaZnAsO reported a semiconducting character with direct band gap and fully occupied Zn *d* states at about −7 eV binding energy.[29] This is of course entirely different from LaFeAsO where the partially filled Fe *d* shell dominates the electronic structure near the Fermi level (E_F), giving rise to metallic features and a tendency toward magnetism. Therefore it may be expected that Zn substitutions will have strong effects on the electronic structure of LaFeAsO, which is in fact what we find.

II. COMPUTATIONAL METHODOLOGY

The present results are based on density functional theory (DFT) supercell calculations. We used $2\times2\times1$ and $2\sqrt{2}\times2\sqrt{2}\times1$ supercells of tetragonal LaFeAsO and replaced one Fe in each cell with Zn. These correspond to $x=0.125$ and 0.0625 in $LaFe_{1-x}Zn_xAsO$, which is reasonably within the range of Zn content realized in the experiment.[21] The experimental lattice parameters at $x=0.1$ ($a=4.038$ Å and $c=8.724$ Å) and 0.05 ($a=4.036$ Å and $c=8.728$ Å) were taken and internal coordinates were fully optimized by total-energy minimization, using the projector augmented wave (PAW) method[30] as implemented in VASP code.[31] The generalized gradient approximation (GGA) of Perdew, Burke, and Ernzerhof (PBE) (Ref. 32) was employed for the exchange-correlation functional. The relaxed structures had somewhat larger bond lengths for Zn-As (~2.5 Å) than for Fe-As (~2.3–2.4 Å). This is somewhat different from the behavior that would be expected in an oxide since the ionic radii of Zn^{2+} and Fe^{2+} are similar and Zn^{2+} is actually slightly

smaller than Fe^{2+}. This may reflect the different chemistry of pnictides and oxides or more likely it may be a consequence of the tendency of nonspin-polarized density functional calculations to place As too close to Fe in these compounds.[33]

We also performed some structure optimizations including relaxation of the lattice parameters. Specifically, we relaxed the structure of LaFeAsO both without magnetism and with the SDW ordering and did the same for our small supercell of composition $LaFe_{0.875}Zn_{0.125}AsO$. For pure LaFeAsO we find, in agreement with previous studies,[33] that the c axis lattice parameter is underestimated in nonmagnetic GGA calculations and that this is improved when SDW order is included. In our GGA calculations, with SDW order, we obtain $a=\sqrt{2}\times 4.073$ Å, $b=\sqrt{2}\times 4.023$ Å, and $c=8.696$ Å while without magnetism our relaxed lattice parameters are $a=4.024$ Å and $c=8.609$ Å. The experimental c-axis lattice parameter is 8.734 Å.[3] In the Zn containing supercell, we again find an interplay between the c axis and magnetism. The calculated c-axis lattice parameter with the SDW order is 8.765 Å, as compared with the result of a nonmagnetic calculation, 8.696 Å.

In any case, once the optimized structures were obtained in the PAW calculations, we used the general potential linearized augmented plane-wave (LAPW) method,[34] with the augmented plane-wave plus local-orbital (APW+LO) implementation of the WIEN2K code,[35,36] to obtain electronic structures and to study magnetism. This was done with the optimized atomic positions and experimental lattice parameters. Proper modeling of strain effects for the disordered alloy would require larger supercells than those employed here but in any case both based on the modest composition dependence of the experimental lattice parameters and the relaxations for the small supercell discussed above these are likely to be small. As in the PAW calculations, we used the PBE-GGA. We used LAPW spheres of radii $2.2a_0$ for La, $1.6a_0$ for O, and $2.1a_0$ for Fe, Zn, and As. The APW+LO basis sets determined by $R_O K_{max} \geq 7$ (K_{max} is the plane-wave cutoff) were used. Convergence of Brillouin-zone sampling was checked by gradually increasing k-point mesh density in self-consistent calculations. Denser meshes were used for density of states (DOS) and magnetic calculations. We did additional magnetic calculations within the local spin-density approximation, which gives weaker magnetic tendencies for the iron pnictides. We also cross-checked our magnetic calculations with the PAW method and obtained consistent results.

Finally, we note that the present calculations were performed using standard density functional theory. As mentioned, there are problems in describing the magnetism of the iron superconductors in this approach. There has been considerable discussion of the nature and role of electronic correlations in these materials. For example, on the one hand signatures of Hubbard bands are remarkably absent in photoemission experiments,[5] a conclusion supported by other spectroscopies.[6] On the other hand, there are clearly important renormalizations of the bands.[5,37–39] Optical experiments, in particular, show a reduction in the Drude weight, demonstrating that there are significant effects of electronic correlations.[39] These may be directly in the charge channel due to Coulomb repulsion, as in cuprates or in the spin channel, i.e., due to spin fluctuations but an explanation based on renormalization due to phonons is excluded. It will be of interest to compare our results with experiment keeping in mind the potential limitations of density functional calculations for these materials. Electronic spectroscopies and their evolution with Zn doping may be particularly useful.

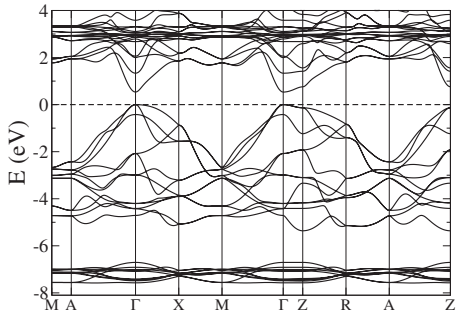

FIG. 1. Calculated band structure of semiconducting LaZnAsO, using the experimental tetragonal lattice parameters $a=4.095$ Å and $c=9.068$ Å (Ref. 40) and optimized internal coordinates ($z_{La}=0.1342$, $z_{As}=0.3271$). The energy zero is chosen at the valence-band maximum.

III. ELECTRONIC STRUCTURE AND MAGNETISM

We start with the electronic structure of the pure Zn compound, LaZnAsO. The electronic band structure and DOS are shown in Figs. 1 and 2, respectively. The results are similar to those reported previously by Bannikov *et al.*[29] It is a semiconductor with direct band gap at Γ, with calculated GGA value of 0.53 eV, which we note is an underestimate as compared to the experimentally determined gap,[26,27] presumably due to DFT errors. The group of low-lying flat bands between −8 and −6 eV, corresponding to the steep peak in DOS, mainly originate from Zn d states. Above −6 eV up to the edge of valence bands, there are 12 bands that derive from O and As p states, with the As p states dominating the upper valence bands. There is only a low As p contribution to the metal derived conduction bands. Therefore Zn occurs as Zn^{2+} in this compound, with minor Zn-As covalency.

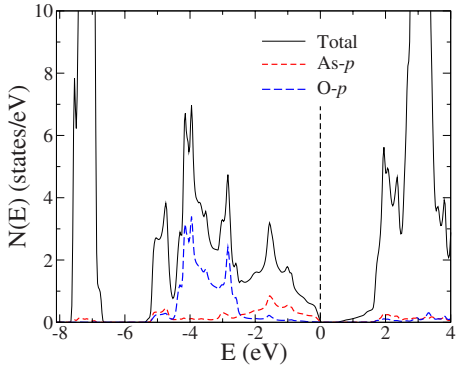

FIG. 2. (Color online) Electronic DOS and projections onto As and O p orbitals within LAPW spheres for LaZnAsO. The contribution from As p state is underestimated due to its spatially extended orbital beyond the LAPW sphere. Total DOS is on a per formula basis and projections per atom.

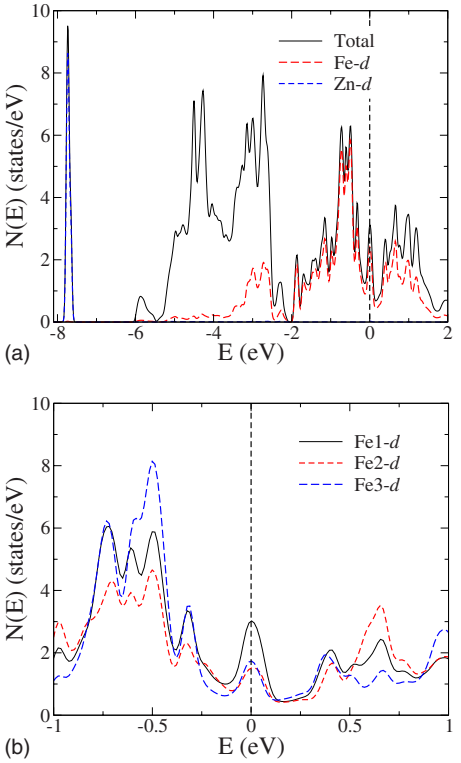

FIG. 3. (Color online) (a) Calculated DOS and projections onto LAPW spheres, on a per formula unit basis for $LaFe_{0.875}Zn_{0.125}AsO$, from the $2\times2\times1$ supercell (see text). The Fermi level is chosen as the energy zero. (b) The *d*-orbital projections of different Fe ions labeled according to the neighbor shell from the Zn in the supercell.

The calculated nonspin-polarized electronic DOS and orbital projections for $LaFe_{0.875}Zn_{0.125}AsO$ are shown in Fig. 3. Comparing with those of LaFeAsO,[4] one can clearly see significant differences due to the Zn alloying in the important energy range around the Fermi level E_F. Similar to the pure Zn compound, LaZnAsO, the Zn *d* levels in Zn-doped LaFeAsO are at high binding energy. They provide the sharp peak in the DOS between −8 and −7.5 eV. Importantly, there is another peak close to E_F, in the pseudogap formed by Fe *d* states in LaFeAsO and other Fe-based materials. Further analysis of projections onto individual Fe sites [Fig. 3(b)] indicates this peak comes mainly from the *d* states of the four Fe atoms nearest to Zn. For other Fe sites, we can also see the peak feature but it is relatively weaker by comparison. It should also be noted that this feature, which represents states induced by Zn substitution, has small but still significant weight on the third-neighbor Fe. This indicates that the interactions between the nearby Zn atoms are still significant in this size supercell (and by implication also in experiment at a doping level of 10%, where there would be many Zn neighbors at distances comparable to those in the supercell). We note that since the peak occurs in a region of finite density of states in the parent compound it is formally a resonance rather a localized defect state. However, considering the narrowness of the feature this distinction may not be important.

Leaving aside this peak induced near E_F and the Zn *d* levels at ~−8 eV, the general shape and features of the DOS

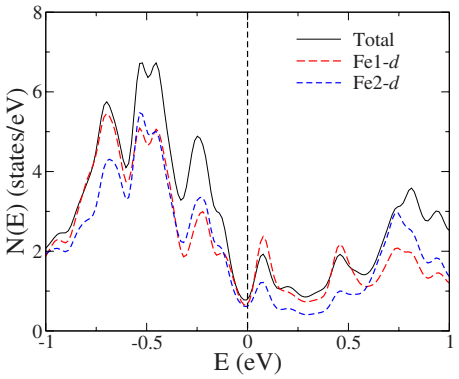

FIG. 4. (Color online) Calculated total DOS and *d* projections for the different Fe sites for $LaFe_{0.9375}Zn_{0.0625}AsO$ (nominal $La_{16}Fe_{15}ZnAs_{16}O_{16}$). For clarity, only the Fe sites up to the second-nearest neighbor to Zn are shown.

for the supercell are rather similar to those of LaFeAsO. In particular, the states near E_F are dominated by Fe *d* orbitals with modest hybridization between Fe *d* and As *p* states.

Figure 4 shows the electronic DOS for the larger supercell of composition $LaFe_{0.9375}Zn_{0.0625}AsO$. As may be seen, the results are generally similar to those obtained for $LaFe_{0.875}Zn_{0.125}AsO$. The Zn *d* states (not shown) are at ~ −8 eV, as in the smaller cell. Importantly, the Zn substitution still induces a sharp Fe *d* peak mainly on the nearest four Fe atoms to the substitutional Zn. The peak in this supercell is slightly above E_F, rather than at E_F as in the smaller cell.

To clarify the nature of the electronic states comprising this peak, we plot the charge-density distribution corresponding to the peak at E_F in the DOS of $LaFe_{0.875}Zn_{0.125}AsO$ (Fig. 3) in Fig. 5. As may be seen, consistent with the Fe *d* projections of the DOS, this state is clearly concentrated on the four Fe atoms nearest to Zn. Besides the fact that the amount of charge on the further neighbor shells is smaller, it is interesting to note that the orbital characters of *d* states

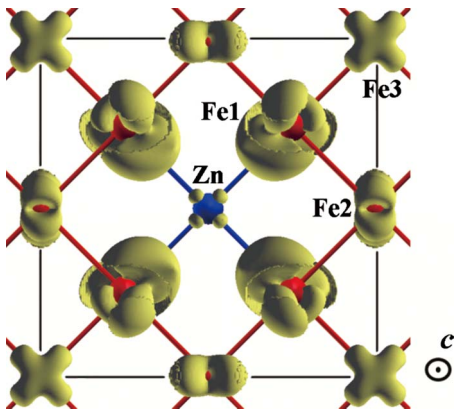

FIG. 5. (Color online) The charge-density distribution corresponding to the DOS peak located at the Fermi level in Fig. 3(a). The isosurface value is chosen as 0.01 e/A^3. Since the peak is mainly dominated by Fe *d* states (with a small contribution from Zn states), only the Fe (Zn) plane (within the supercell employed) is shown. The Fe and Zn atoms are marked as red and blue spheres, respectively.

TABLE I. Calculated moments (in μ_B) of Fe for the ground-state magnetic order of the two supercells investigated, using both local-density approximation (LDA) and GGA exchange-correlation functionals. The order of numbers refers to the distance of the Fe atoms from Zn in terms of near-neighbor shells. Note that in the calculations, the system without Zn is also magnetic with SDW order as the ground state and other competing orders as well. The large moments on the distant Fe atoms, especially in GGA calculations reflect this and are not directly a consequence of the Zn.

		First	Second	Third	Fourth	Fifth
$LaFe_{0.875}Zn_{0.125}AsO$	LDA	+0.8	−0.7	−0.3		
	GGA	+1.5	−1.5	−1.3		
$LaFe_{0.9375}Zn_{0.0625}AsO$	LDA	+0.7	−0.6	+0.3	−0.3	+0.7
	GGA	+1.8	−1.4	+1.5	−1.1	+1.7

involved on the different Fe sites varies. For the nearest-neighbor Fe, the states involved have primarily d_{xy} and d_{z^2} characters while the second-neighbor contribution is from d_{xz}/d_{yz} states and the third-neighbor contribution has $d_{x^2-y^2}$ and d_{z^2} characters.

While nonspin-polarized calculations show a sharp peak in the DOS at or near E_F in the supercells, such a situation clearly cannot be stable. Spin-polarized calculations show in fact that the feature leads to the formation of a moment that splits the peak. This moment is spread over the four Fe atoms around the nearest-neighbor Zn. Since these atoms are second neighbors of each other on the square lattice, a parallel spin arrangement of them corresponds to the pattern of the checkerboard antiferromagnetic (nearest-neighbor antiferromagnetism) state, which is a state that competes with the SDW in the Fe-based superconductors. This disruption of the SDW is seen in both supercells and in both GGA and LSDA calculations (Table I, note that while especially in the GGA calculations there are large moments on far neighbors from the Zn, these do not have the same pattern as the SDW, which is the ground state without Zn; this shows the disruption of the SDW while at the same time reflecting the tendency of the Fe atoms to have moments in GGA calculations, regardless of the magnetic order; the details of the Fe spin arrangements around the Zn atom are no doubt sensitive to the particular arrangement of Zn atoms).

IV. SUMMARY AND DISCUSSION

Thus we find two mechanisms by which Zn doping works against the SDW. First of all, it introduces localized states, disrupting the electronic structure of the Fe sheets near E_F. This will be destructive to the Fermi-surface nesting. Second, and perhaps more importantly, it introduces local moments that have the pattern of the checkerboard antiferromagnetic state mainly on the four neighboring Fe. This may then lead to a spin glass as opposed to the paramagnetic metallic state with spin fluctuations that is characteristic of the clean materials when the SDW is destroyed by doping or pressure. Within this scenario, the resulting phase would not be a conventional semiconductor with a band gap but more likely an insulator where the insulating character comes from Anderson localization associated with the strong scattering in the spin glass. Localization would be favored in the SDW state because of the low carrier density in that state and also in the precursor orthorhombic phase between the SDW ordering and the somewhat higher temperature structural transition. This is consistent with observations in the FeSe system upon Cu doping, in particular, the observation of local moments in proximity to Cu in the Cu-doped FeSe,[22] which has a structural transition but not the SDW transition when undoped.

This does not provide a clear explanation of why Zn doping has only a small effect on the superconductivity. One might begin speculating by observing that the carrier density in the doped samples is higher, which would work against Anderson localization and second that within an Eliashberg framework with spin fluctuations as a pairing mechanism, superconductivity depends on an integral over the Fermi surface of the pairing interaction related to the real part of the susceptibility.[41] This means that the strength of the pairing for an $s(+/-)$ state, which is regarded as a highly likely state for these materials, would depend on an average over a volume of momentum space related to the Fermi-surface size while SDW ordering would depend on the value at the nesting vector. Thus, within a picture where the superconductivity arises from spin fluctuations, fluctuations over a region of the Brillouin zone around the zone corner and not just at the zone corner, will be pairing (see, for example, the discussion in Ref. 42). Because of this, the frustrating effect of local checkerboard type moments around Zn could be smaller for superconductivity than for the SDW itself. However, this explanation seems rather contrived and in fact the destruction of the SDW state in the undoped compound at low Zn concentrations would presumably then result in the metallic state rather than an insulator as observed. Therefore the explanation may in fact be in the difference between samples reported in Ref. 21 which were doped with F and those of Guo *et al.*,[25] who found a strong suppression of superconductivity with Zn in samples doped by O vacancies. Considering the phase separation observed at modest Zn concentrations and the high affinity of Zn for F it will be useful to verify that Zn actually substitutes for Fe in bulk LaFeAs(O,F) samples rather than entering the lattice in some other way. In any case, it will be interesting to further examine Zn-doped

samples experimentally to look for the predicted moments on the nearest-neighbor Fe sites and to determine whether the characteristics of the insulating Zn-doped phase are indicative of a true semiconductor or of an Anderson localized system.

ACKNOWLEDGMENTS

We are grateful for helpful discussions with M. H. Du and C. Felser. This work was supported by the Department of Energy, Division of Materials Sciences and Engineering.

[1] Y. Kamihara, T. Watanabe, M. Hirano, and H. Hosono, J. Am. Chem. Soc. **130**, 3296 (2008).
[2] G. F. Chen, Z. Li, D. Wu, G. Li, W. Z. Hu, J. Dong, P. Zheng, J. L. Luo, and N. L. Wang, Phys. Rev. Lett. **100**, 247002 (2008).
[3] C. de la Cruz, Q. Huang, J. W. Lynn, J. Li, W. Ratcliff II, J. L. Zarestky, H. A. Mook, G. F. Chen, J. L. Luo, N. L. Wang, and P. Dai, Nature (London) **453**, 899 (2008).
[4] D. J. Singh and M. H. Du, Phys. Rev. Lett. **100**, 237003 (2008).
[5] D. H. Lu, M. Yi, S. K. Mo, A. S. Erickson, J. Analytis, J. H. Chu, D. J. Singh, Z. Hussain, T. H. Geballe, I. R. Fisher, and Z.-X. Shen, Nature (London) **455**, 81 (2008).
[6] W. L. Yang, A. P. Sorini, C. C. Chen, B. Moritz, W. S. Lee, F. Vernay, P. Olalde-Velasco, J. D. Denlinger, B. Delley, J. H. Chu, J. G. Analytis, I. R. Fisher, Z. A. Ren, J. Yang, W. Lu, Z. X. Zhao, J. van den Brink, Z. Hussain, Z.-X. Shen, and T. P. Devereaux, Phys. Rev. B **80**, 014508 (2009).
[7] S. E. Sebastian, J. Gillett, N. Harrison, P. H. C. Lau, D. J. Singh, C. H. Mielke, and G. G. Lonzarich, J. Phys.: Condens. Matter **20**, 422203 (2008).
[8] G. Xiao, M. Z. Cieplak, A. Gavrin, F. H. Streitz, A. Bakhshai, and C. L. Chien, Phys. Rev. Lett. **60**, 1446 (1988).
[9] G. Xiao, M. Z. Cieplak, J. Q. Xiao, and C. L. Chien, Phys. Rev. B **42**, 8752 (1990).
[10] S. Zagoulaev, P. Monod, and J. Jegoudez, Phys. Rev. B **52**, 10474 (1995).
[11] A. S. Sefat, A. Huq, M. A. McGuire, R. Jin, B. C. Sales, D. Mandrus, L. M. D. Cranswick, P. W. Stephens, and K. H. Stone, Phys. Rev. B **78**, 104505 (2008).
[12] A. S. Sefat, R. Jin, M. A. McGuire, B. C. Sales, D. J. Singh, and D. Mandrus, Phys. Rev. Lett. **101**, 117004 (2008).
[13] A. Leithe-Jasper, W. Schnelle, C. Geibel, and H. Rosner, Phys. Rev. Lett. **101**, 207004 (2008).
[14] L. J. Li, Y. K. Luo, Q. B. Wang, H. Chen, Z. Ren, Q. Tao, Y. K. Li, X. Lin, M. He, Z. W. Zhu, G. H. Cao, and Z. A. Xu, New J. Phys. **11**, 025008 (2009).
[15] S. Paulraj, S. Sharma, A. Bharathi, A. T. Satya, S. Chandra, Y. Hariharan, and C. S. Sundar, arXiv:0902.2728 (unpublished).
[16] F. Han, X. Zhu, P. Cheng, G. Mu, Y. Jia, L. Fang, Y. Wang, H. Luo, B. Zeng, B. Shen, L. Shan, C. Ren, and H.-H. Wen, Phys. Rev. B **80**, 024506 (2009).
[17] W. Schnelle, A. Leithe-Jasper, R. Gumeniuk, U. Burkhardt, D. Kasinathan, and H. Rosner, Phys. Rev. B **79**, 214516 (2009).
[18] Y. Qi, L. Wang, Z. Gao, D. Wang, X. Zhang, Z. Zhang, and Y. Ma, Phys. Rev. B **80**, 054502 (2009).
[19] L. Zhang and D. J. Singh, Phys. Rev. B **79**, 174530 (2009).
[20] P. L. Alireza, Y. T. C. Ko, J. Gillett, C. M. Petrone, J. M. Cole, G. G. Lonzarich, and S. E. Sebastian, J. Phys.: Condens. Matter **21**, 012208 (2009).
[21] Y. Li, X. Lin, Q. Tao, C. Wang, T. Zhou, L. Li, Q. Wang, M. He, G. Cao, and Z. Xu, New J. Phys. **11**, 053008 (2009).
[22] A. J. Williams, T. M. McQueen, V. Ksenofontov, C. Felser, and R. J. Cava, J. Phys.: Condens. Matter **21**, 305701 (2009).
[23] M. K. Wu, F. C. Hsu, K. W. Yeh, T. W. Huang, J. Y. Luo, M. J. Wang, H. H. Chang, T. K. Chen, S. M. Rao, B. H. Mok, C. L. Chen, Y. L. Huang, C. T. Ke, P. M. Wu, A. M. Chang, C. T. Wu, and T. P. Perng, Physica C **469**, 340 (2009).
[24] T. W. Huang, T. K. Chen, K. W. Yeh, C. T. Ke, C. L. Chen, Y. L. Huang, F. C. Hsu, M. K. Wu, P. M. Wu, M. Avdeev, and A. Studer, arXiv:0907.4001 (unpublished).
[25] Y. F. Guo, Y. G. Shi, V. P. S. Awana, S. Yu, A. A. Belik, Y. Matsushita, M. Tanaka, K. Katsuya, K. Kobayashi, K. Yamaura *et al.*, arXiv:0911.2975 (unpublished).
[26] H. Lincke, R. Glaum, V. Dittrich, M. H. Moller, and R. Pottgen, Z. Anorg. Allg. Chem. **635**, 936 (2009).
[27] K. Kayanuma, R. Kawamura, H. Hiramatsu, H. Yanagi, M. Hirano, T. Kamiya, and H. Hosono, Thin Solid Films **516**, 5800 (2008).
[28] K. Kayanuma, H. Hiramatsu, M. Hirano, R. Kawamura, H. Yanagi, T. Kamiya, and H. Hosono, Phys. Rev. B **76**, 195325 (2007).
[29] V. V. Bannikov, I. R. Shein, and A. L. Ivanovskii, Mater. Chem. Phys. **116**, 129 (2009).
[30] G. Kresse and D. Joubert, Phys. Rev. B **59**, 1758 (1999).
[31] G. Kresse and J. Furthmüller, Phys. Rev. B **54**, 11169 (1996).
[32] J. P. Perdew, K. Burke, and M. Ernzerhof, Phys. Rev. Lett. **77**, 3865 (1996).
[33] I. I. Mazin, M. D. Johannes, L. Boeri, K. Koepernik, and D. J. Singh, Phys. Rev. B **78**, 085104 (2008).
[34] D. J. Singh and L. Nordstrom, *Planewaves, Pseudopotentials and the LAPW Method*, 2nd ed. (Springer-Verlag, Berlin, 2006).
[35] P. Blaha, K. Schwarz, G. Madsen, D. Kvasnicka, and J. Luitz, WIEN2K, *An Augmented Plane* Wave+Local *Orbitals Program for Calculating Crystal Properties* (K. Schwarz, Technical Univiversity, Wien, Austria, 2001).
[36] E. Sjöstedt, L. Nordstrom, and D. J. Singh, Solid State Commun. **114**, 15 (2000).
[37] A. I. Coldea, J. D. Fletcher, A. Carrington, J. G. Analytis, A. F. Bangura, J. H. Chu, A. S. Erickson, I. R. Fisher, N. E. Hussey, and R. D. McDonald, Phys. Rev. Lett. **101**, 216402 (2008).
[38] M. Yi, D. H. Lu, J. G. Analytis, J. H. Chu, S. K. Mo, R. H. He, M. Hashimoto, R. G. Moore, I. I. Mazin, D. J. Singh, Z. Hussain, I. R. Fisher, and Z.-X. Shen, Phys. Rev. B **80**, 174510 (2009).
[39] M. M. Qazilbash, J. J. Hamlin, R. E. Baumbach, L. Zhang, D. J. Singh, M. B. Maple, and D. N. Basov, Nat. Phys. **5**, 647 (2009).
[40] A. T. Nientiedt and W. Jeitschko, Inorg. Chem. **37**, 386 (1998).
[41] I. I. Mazin, D. J. Singh, M. D. Johannes, and M. H. Du, Phys. Rev. Lett. **101**, 057003 (2008).
[42] D. J. Singh, Phys. Rev. B **78**, 094511 (2008).